

# High-Frequency Characteristics of Metal/Native-Oxide Multilayers

G. S. D. Beach, T. J. Silva, F. T. Parker, and A. E. Berkowitz

**Abstract**—The high-frequency magnetization dynamics of magnetically soft  $\text{Co}_x\text{Fe}_{100-x}$  metal/native-oxide multilayers were studied as a function of alloy composition ( $10 \leq x \leq 50$ ) using a time-domain inductive technique. The data show intrinsic resonance frequencies ranging from 2.1 to 3.7 GHz due to the variation of anisotropy field with  $x$ . The frequencies are consistent with a simple ferromagnetic resonance (FMR) response, with the dynamical anisotropy field equal to the static anisotropy field. The large dc permeabilities, ranging from 200 to 1000, are therefore maintained at high frequency. The combination of high permeability, high resonance frequency, low damping, and a tunable anisotropy field, along with a high resistivity, make this system ideally suited to high-frequency applications.

**Index Terms**—High-frequency magnetization dynamics, high-permeability thin films, soft magnetic materials.

## I. INTRODUCTION

THERE is strong demand in the magnetic recording industry for new high-permeability materials with operating frequencies in the gigahertz regime for applications such as heads, shields, and soft underlayers. Two principal parameters for high-frequency applications are permeability and resonance frequency. For a uniaxial material with anisotropy field  $H_k$  and saturation magnetization  $M_s$ , the (dc) hard-axis permeability is given by

$$\mu_{dc} = \frac{M_s}{H_k}. \quad (1)$$

In the absence of excessive damping or eddy-current screening, the bandwidth is determined by the ferromagnetic resonance (FMR) frequency

$$f_{\text{FMR}} = \frac{g\mu_B}{h} \sqrt{M_s H_k} \quad (2)$$

where  $g$  is the spectroscopic splitting (Landé) factor. Relations (1) and (2) reveal an inherent trade-off between permeability and bandwidth; increasing  $\mu_{dc}$  by decreasing  $H_k$  inevitably leads to a lower maximum operating frequency. The ability to easily “tune”  $H_k$  (and thus optimize  $\mu_{dc}$  and  $f_{\text{FMR}}$ ) for a particular application is therefore attractive. The  $\text{Co}_x\text{Fe}_{100-x}$  metal/native-oxide multilayer (MNOM) consisting of repeats of 2.0-nm metal layers separated by high-resistivity native

oxide layers has recently been shown to have excellent soft magnetic properties and an anisotropy field that varies almost linearly with  $x$  for  $0 \leq x \leq 90$  [1].  $M_s$  is also large (up to 1350 kA/m) because although a significant volume of the MNOM is oxide, the native oxide is magnetic and contributes to  $M_s$  [2]. Based on reported [1] values of  $H_k$  and  $M_s$ , (1) and (2) predict resonance frequencies ranging from 1.3 to 5.6 GHz, and permeabilities from 1400 to 50 as  $x$  is increased from 0 to 90.

This paper presents a study of the high-frequency magnetization dynamics in the MNOM system over a range of alloy composition, using pulsed inductive microwave magnetometry (PIMM) [3], [4]. We find that the frequency response is amenable to fitting with the Kittel equation, and the native oxide layers do not overly damp the dynamic response. In addition, the high-frequency permeability and resonance frequency agree well with predictions based on values of  $H_k$  and  $M_s$  obtained through quasistatic measurements.

## II. EXPERIMENTAL DETAILS

MNOMs were sputtered at room temperature onto Si and polished Corning 7059 glass substrates using  $\text{Co}_x\text{Fe}_{100-x}$  alloy targets, as described in [1]. Multilayers were produced by repeatedly depositing a nominal thickness  $t_0$  of  $\text{Co}_x\text{Fe}_{100-x}$  and exposing the layer *in situ* to oxygen ( $\sim 1 \times 10^{-2}$  Pa for 10 s) to form metal/native-oxide bilayers. A multilayer containing  $N$  such bilayers is denoted  $[\text{Co}_x\text{Fe}_{100x}(t_0)/\text{oxide}]_N$ . A dc field of  $\sim 8$  kA/m ( $\sim 100$  Oe) applied in the plane of the substrate during deposition induced a uniaxial anisotropy along the field direction. MNOMs of  $\text{Co}_x\text{Fe}_{100-x}$  compositions  $x = 10, 30,$  and  $50$  were studied, with  $t_0 = 2$  nm and  $N = 50$ .

Previous work [1], [2] has shown that samples similarly produced have a regular layered structure, with  $\sim 1.2$ -nm metal layers and  $\sim 1.2$ -nm oxide layers (including dilation due to the oxidation). The total thickness of the present samples is thus  $\sim 120$  nm. A vibrating sample magnetometer (VSM) was used for magnetic characterization. The hysteresis loops (see Fig. 1) show a well-defined uniaxial anisotropy, with a square, high-remanence easy-axis loop and a linear, low-coercivity hard-axis loop. No significant differences were found between samples deposited on Si and glass. The easy-axis coercivity was  $\sim 880$  A/m (11 Oe) for each sample, and the anisotropy field  $H_k$  increased from 1.6 kA/m (20 Oe) for  $x = 10$  to 7 kA/m (88 Oe) for  $x = 50$  (see Fig. 4). For  $x = 30$  and  $x = 50$ , the hard-axis loop was nearly closed, with a hard-axis coercivity  $H_{ch} < 80$  A/m (1 Oe) ( $H_{ch}/H_k < 0.02$ ), while the hard-axis loop for the  $x = 10$  sample was somewhat more open ( $H_{ch} = 112$  A/m or  $H_{ch}/H_k = 0.07$ ).

Manuscript received January 6, 2003. This work was supported in part by the National Institute of Standards and Technology’s Nanotechnology Initiative.

G. S. D. Beach, F. T. Parker, and A. E. Berkowitz are with the Department of Physics and the Center for Magnetic Recording Research, University of California, San Diego, La Jolla, CA 92093-0401 USA (e-mail: gbeach@physics.ucsd.edu).

T. J. Silva is with the National Institute of Standards and Technology, Boulder, CO 80303 USA.

Digital Object Identifier 10.1109/TMAG.2003.815551

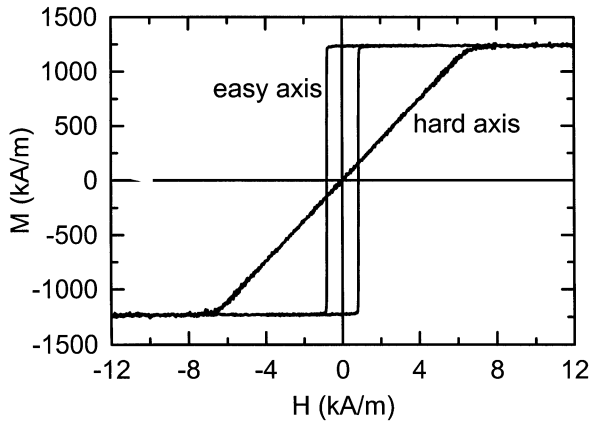


Fig. 1. In-plane hysteresis loops for  $[\text{Co}_{50}\text{Fe}_{50} (2.0 \text{ nm})/\text{oxide}]_{50}/\text{Si}$ .

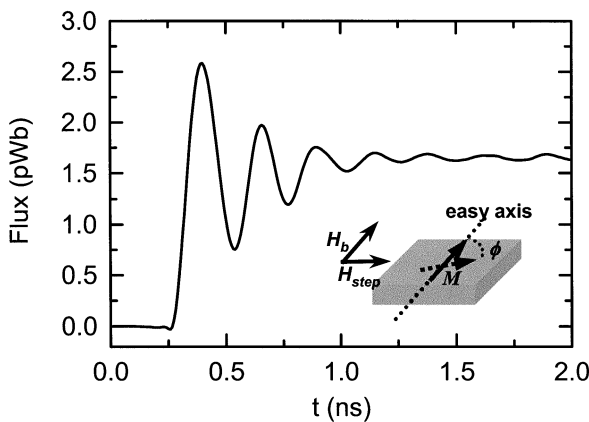


Fig. 2. Example of the magnetization response of  $[\text{Co}_{50}\text{Fe}_{50} (2.0\text{nm})/\text{oxide}]_{50}/\text{glass}$  to a field step, with a bias field  $H_b = 960 \text{ A/m}$  (12 Oe). Measurement geometry is shown in the inset.

Inductive measurements were performed as described in detail by Silva *et al.* [3], using PIMM [4]. Field-step excitations were applied along the hard axis with a coplanar waveguide driven by 10-V pulses with a 55-ps rise time and 10-ns duration. The resulting field step had a magnitude of  $\sim 200 \text{ A/m}$  (2.5 Oe) [3]. The instrument bandwidth is greater than 10 GHz, as determined by the pulse rise time [4], and was sufficient to accommodate the response of the present samples [5]. The step response of the sample magnetization was measured through the inductive coupling of the time-dependent sample flux along the field-step direction to the waveguide.

### III. RESULTS AND DISCUSSION

In response to a hard-axis field step (see Fig. 2), the sample rotates toward and performs damped precession about the new equilibrium magnetization angle  $\phi_0$ , according to [3]

$$\phi(t) = \phi_0 + \beta_0 \sin(2\pi f_p t + \varphi) e^{-t/\tau}. \quad (3)$$

Here,  $\beta_0$  and  $\varphi$  are the amplitude and phase, respectively, of the oscillations. The damping time constant  $\tau$  is related to the dimensionless Gilbert damping parameter  $\alpha$  by

$$\alpha = \frac{2\hbar}{g\mu_B\mu_0 M_s \tau}. \quad (4)$$

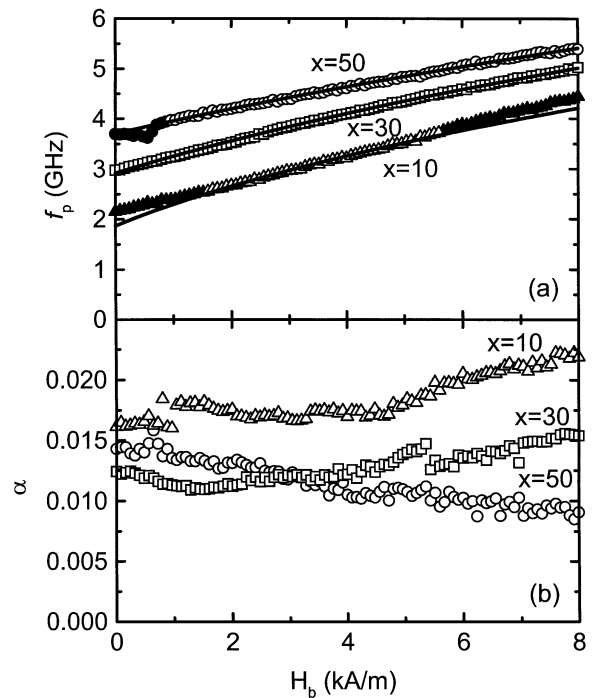


Fig. 3. (a) Precessional frequency and (b) damping parameter as a function of bias field for  $[\text{Co}_x\text{Fe}_{100-x} (2.0 \text{ nm})/\text{oxide}]_{50}$ , with  $x = 10, 30$ , and  $50$ . Solid lines in (a) are fits to (5), with the filled symbols excluded from the fits.

For weak damping, the precessional frequency  $f_p$  is expected to follow the Kittel equation

$$f_p = \frac{g\mu_B}{h} \sqrt{M_{\text{eff}}(H_k^d + H_b)} \quad (5)$$

where  $H_b$  is a dc bias field applied along the easy axis, and  $H_k^d$  is the *dynamic* anisotropy field, which is not necessarily equal to the static (dc) value [6].  $M_{\text{eff}}$  provides the demagnetizing field driving the precession and includes contributions from both  $M_s$  and any surface anisotropy.  $M_{\text{eff}}$  was determined from the perpendicular anisotropy field  $H_k^\perp$  via  $M_{\text{eff}} = H_k^\perp$  to be 1970, 1590, and 1430 kA/m for  $x = 10, 30$ , and  $50$ , respectively. The relation of  $M_{\text{eff}}$  to  $M_s$  and the possible role of surface anisotropy associated with the metal/oxide interfaces is currently under study.

A fit of the step response to (3) allows extraction of  $f_p$  and  $\alpha$ , whereas the bias-field dependence of  $f_p$  provides both  $H_k^d$  and  $g$  through (5). Fig. 3 shows the dependence of  $f_p$  and  $\alpha$  on  $H_b$  for the three compositions studied. For  $x = 50$  and  $x = 30$ , the  $f_p$  data are well fitted by (5), although some discrepancy is found for the  $x = 50$  data below  $H_b = H_{ce} = 880 \text{ A/m}$  (11 Oe). The zero-bias precessional frequency compares well with the FMR frequency calculated from (2) (with  $g = 2$  and  $M_s = M_{\text{eff}}$ ), as shown in Fig. 4(a), whereas the dynamic anisotropy field is nearly equal to the static value (obtained from VSM measurements) for these compositions [Fig. 4(b)]. The  $x = 10$  data in Fig. 3(a) deviate more significantly from a simple FMR response, with an enhanced precessional frequency in both the low and high bias-field regimes. The source of this behavior is unclear and may be related to increased coupling to spin-wave modes for this sample. This makes the fitted parameters ( $H_k^d$  and  $g$ ) in (5) less meaningful for this particular sample, as is

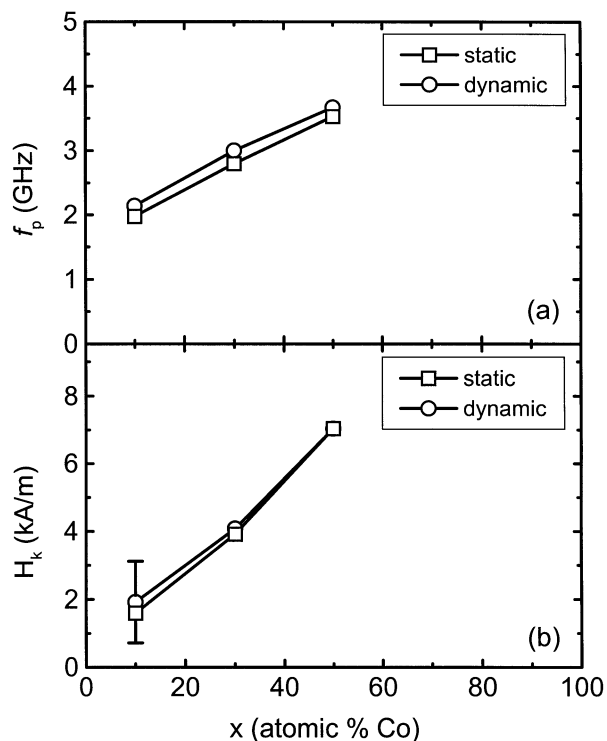


Fig. 4. (a) Intrinsic precessional frequency ( $H_b = 0$ ) and (b) anisotropy field for  $[\text{Co}_x\text{Fe}_{100-x}(2.0 \text{ nm})/\text{oxide}]_{50}$  as a function of  $x$ . The results of dynamic measurements are compared with static values, where the “static”  $f_p$  was calculated from the Kittel equation using the static  $H_k$  (see text). Error bars are smaller than the symbol size except where noted.

reflected in the error bar in Fig. 4(b). The error bar spans the range of  $H_k^d$  obtained by fitting (5) to different  $H_b$  regions in Fig. 3(a). The overall close correspondence between the dynamical anisotropy and the static value in these samples indicates that the intrinsic dynamics driving the precession do not vary up to the precessional frequency.

The low damping constants of these MNOM samples [see Fig. 3(b)], which are similar to values found in Permalloy [7], are quite favorable for high-frequency response. The complicated nature of the microstructure, including exchange interaction at the metal/oxide interface, does not introduce any excessive damping mechanisms that might limit the performance at high frequencies. The damping constant depends weakly on bias field for all samples, possibly related to a weak dependence on resonance frequency, which itself varies with  $H_b$ . The monotonic decrease of  $\alpha$  with increasing  $H_b$  seen for  $x = 50$  has also been observed in Permalloy [3] and FeTaN [5].

Fitting (5) to the data of Fig. 3(a) also provides the effective  $g$  factor, although it is not independent of  $M_{\text{eff}}$  in the fitting. The fits yield  $g = 2.10$  and  $g = 2.04$  for  $x = 50$  and  $x = 30$ , respectively, which are reasonable values for CoFe alloy-based thin films [8]. The fit for  $x = 10$  in the region indicated in Fig. 3(a) gives  $g = 1.71$ , which is quite low. However, as mentioned, (5) does not adequately describe the response for this sample.

#### IV. CONCLUSION

A study of the compositional dependence of the high-frequency response of  $\text{Co}_x\text{Fe}_{100-x}$  MNOMs has been presented. The dynamics are consistent with a simple FMR response, although some deviation from the Kittel equation is found in the bias-field dependence of the most Fe-rich composition. The anisotropy field, and thus the permeability and precessional frequency, are easily varied with composition. Intrinsic precessional frequencies (with  $H_b = 0$ ) from 2.1 to 3.7 GHz were observed in samples with  $10 \leq x \leq 50$ , with the dynamical anisotropy fields corresponding closely to the static values. Underdamped response was measured for all samples, permitting use of MNOM systems in high-frequency applications.

#### REFERENCES

- [1] G. S. D. Beach, A. E. Berkowitz, F. T. Parker, and D. J. Smith, “Magnetically-soft, high-moment, high resistivity thin films using discontinuous metal/native oxide multilayers,” *Appl. Phys. Lett.*, vol. 79, p. 224, May 2001.
- [2] G. S. D. Beach, V. G. Harris, F. T. Parker, B. Ramadurai, D. J. Smith, and A. E. Berkowitz, “Magnetic properties of the native oxide in metal/native oxide multilayers,” *J. Appl. Phys.*, vol. 91, pp. 7526–7528, June 2002.
- [3] T. J. Silva, C. S. Lee, T. M. Crawford, and C. T. Rogers, “Inductive measurement of ultrafast magnetization dynamics in thin-film Permalloy,” *J. Appl. Phys.*, vol. 85, pp. 7849–7862, June 1999.
- [4] A. B. Kos, T. J. Silva, and P. Kabos, “Pulsed inductive microwave magnetometer,” *Rev. Sci. Instrum.*, vol. 73, pp. 3563–3569, Oct. 2002.
- [5] C. Alexander Jr., J. Rantschler, T. J. Silva, and P. Kabos, “Frequency- and time-resolved measurements of FeTaN films with longitudinal bias fields,” *J. Appl. Phys.*, vol. 87, pp. 6633–6635, May 2000.
- [6] R. Lopusnik, J. P. Nibarger, T. J. Silva, and Z. Celinski, “Different dynamic and static magnetic anisotropy in thin Permalloy films,” *Appl. Phys. Lett.*, vol. 83, p. 96, July 2003.
- [7] C. E. Patton, “Linewidth and relaxation processes for the main resonance in the spin-wave spectra of Ni-Fe alloy films,” *J. Appl. Phys.*, vol. 39, pp. 3060–3068, June 1968.
- [8] F. Schreiber, J. Pflaum, Z. Frait, T. Mühge, and J. Pelzl, “Gilbert damping and  $g$ -factor in  $\text{Fe}_x\text{Co}_{1-x}$  alloy films,” *Solid-State Commun.*, vol. 93, pp. 965–968, Mar. 1995.